iScience

CellPress
OPEN ACCESS

Article

A Major Change in Rate of Climate Niche Envelope Evolution during Hominid History

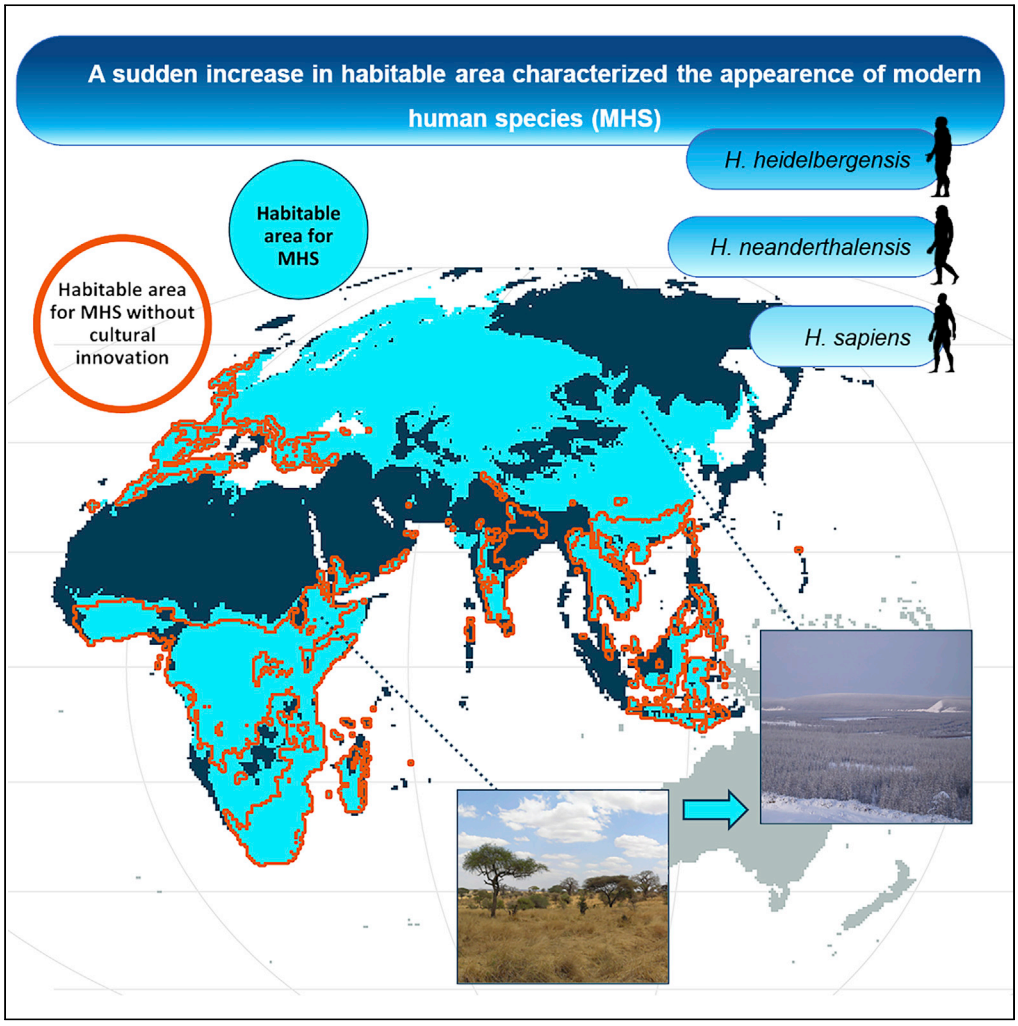

Alessandro Mondanaro, Marina Melchionna, Mirko Di Febbraro, ..., Penny Spikins, Antonio Profico, Pasquale Raia

pasquale.raia@unina.it

HIGHLIGHTS

Homo sapiens oversteps our ecological niche limits by means of culture

The origin of *Homo* niche-construction ability is unknown

We found *Homo* species other than *H. sapiens* were able to construct their own niche

Mondanaro et al., iScience *23*, 101693
November 20, 2020
https://doi.org/10.1016/j.isci.2020.101693

iScience

CellPress
OPEN ACCESS

Article

A Major Change in Rate of Climate Niche Envelope Evolution during Hominid History

Alessandro Mondanaro,[1,2] Marina Melchionna,[1] Mirko Di Febbraro,[3] Silvia Castiglione,[1] Philip B. Holden,[4] Neil R. Edwards,[4] Francesco Carotenuto,[1] Luigi Maiorano,[5] Maria Modafferi,[1] Carmela Serio,[6] Josè A.F. Diniz-Filho,[7] Thiago Rangel,[7] Lorenzo Rook,[2] Paul O'Higgins,[8] Penny Spikins,[8] Antonio Profico,[8] and Pasquale Raia[1,9,*]

SUMMARY

***Homo sapiens* is the only species alive able to take advantage of its cognitive abilities to inhabit almost all environments on Earth. Humans are able to culturally construct, rather than biologically inherit, their occupied climatic niche to a degree unparalleled within the animal kingdom. Precisely, when hominins acquired such an ability remains unknown, and scholars disagree on the extent to which our ancestors shared this same ability. Here, we settle this issue using fine-grained paleoclimatic data, extensive archaeological data, and phylogenetic comparative methods. Our results indicate that whereas early hominins were forced to live under physiologically suitable climatic conditions, with the emergence of *H. heidelbergensis*, the *Homo* climatic niche expanded beyond its natural limits, despite progressive harshening in global climates. This indicates that technological innovations providing effective exploitation of cold and seasonal habitats predated the emergence of *Homo sapiens*.**

INTRODUCTION

The genus *Homo* has existed for some three million years (Harmand et al., 2015; Villmoare et al., 2015). For one third of this stretch of time, human species were confined to tropical and sub-tropical Africa, which is the homeland of the genus (Carotenuto et al., 2016; Lordkipanidze et al., 2007) and is rich in the warm, savanna-like environments to which most early hominins were best adapted (Lee-Thorp et al., 2010; White et al., 2009). With the emergence of *Homo erectus* some 2 Ma ago, *Homo* began to disperse outside of Africa but remained confined to low latitudes, possibly because of physiological limits to cold tolerance (Dunbar et al., 2014) combined with the inevitable constraints of biogeographical barriers and habitat variability. However, later *Homo* species were able to expand their distribution to Northern Europe and Western Siberia, even as the contemporaneous establishment of full glacial cycles was making global temperatures colder than ever before during the history of the genus. Findings in Happisburgh and Pakefield (UK) date the earliest occurrence of *Homo* at the southern edge of the boreal zone at some 0.7–0.9 Ma (Parfitt et al., 2010). The occupation of such northern temperate and boreal zones presents a number of notable challenges. Not only was the cold itself challenging for hominins physiologically adapted to African climates but also seasonality imposes extreme annual resource fluctuations, which imply a reliance on hunted meat for survival (Pearce et al., 2014). Adaptations facilitating survival in cold environments may have included the use of fire, shelters or clothing, weapons useful to bring down large game species (Thieme, 1997), as well as extended social networks, with vulnerable infants being particularly susceptible to mortality (Spikins et al., 2019; Martin et al., 2020).

Unfortunately, clothing manufacturing leaves very little in the way of fossil remains (Hosfield, 2016). The first microwear evidence of hide scraping (for manufacturing clothes) at Hoxne (UK), Biâche-Saint-Vaast, Pech de l'Azé and Abri Peyrony (France), and Shöningen (Germany) (d'Errico and Henshilwood, 2007; Gilligan, 2010; Henshilwood et al., 2002) is just some 50 ka old at the most (Kittler et al., 2003; Gilligan, 2007). Only the two most recent human species, *H. neanderthalensis* and *H. sapiens*, left incontrovertible evidence that they were able to produce complex, cold-proof clothing at that time. To make things more complex, in the particular case of *H. neanderthalensis*, biological adaptation, besides material culture, was possibly involved in their ability to withstand the cold. *H. neanderthalensis* possessed relatively short limbs,

[1]Department of Earth, Environmental and Resources Sciences, University of Naples "Federico II", Naples 80126, Italy

[2]Department of Earth Science. University of Florence, Florence 50121, Italy

[3]Department of Bioscience and Territory. University of Molise, Pesche, Isernia 86090, Italy

[4]School of Environment, Earth and Ecosystem Sciences, The Open University, Milton Keynes MK7 6BJ, UK

[5]Department of Biology and Biotechnologies Charles Darwin, University of Rome La Sapienza, Rome 00185, Italy

[6]Research Centre in Evolutionary Anthropology and Palaeoecology, School of Biological and Environmental Sciences, Liverpool John Moores University, Liverpool L3 3AF, UK

[7]Department of Ecology, ICB, Universidade Federal de Goiás, Goiânia 74968-755, Brasil

[8]Department of Archaeology and Hull York Medical School, University of York, York YO10 5DD, UK

[9]Lead Contact

*Correspondence: pasquale.raia@unina.it

https://doi.org/10.1016/j.isci.2020.101693

and a large midface and nasal cavity proposed to be specific cold adaptations, to heat and humidify inspired air, although the issue is far from resolved and there is evidence for the contrary (Rae et al., 2011; Benito et al., 2017; Wroe et al., 2018). In contrast to any other *Homo*, *H. sapiens* is considered the only species in the genus able to occupy cold regions through a genuinely cultural process, driven by our technology, including the mastering of fire, ever improving clothing craftsmanship, and construction of shelters (Boivin et al., 2016; Gilligan, 2010; Hiscock, 2013; Laland et al., 2001). The archaeological record of *Homo sapiens* shows our own species was able to construct its own niche, using technologies transmitted over large regions and across generations via cultural interactions. *Homo sapiens* could thus exploit climatic variability over time and space, rather than being physiologically limited by it (Banks et al., 2006, 2008, 2011, 2013; Dunbar et al., 2014; Spikins et al., 2019; Nicholson, 2019; Xu et al., 2020).

This view sets *H. sapiens* apart from any other human species in terms of cognitive skills and implicitly rejects the idea that older *Homo* may have had sufficiently modern material culture to overcome climatic harshness (Roberts and Stewart, 2018). With such a poor fossil record of clothes and tools to produce them and because of great uncertainty about deep past local paleoclimates and human dispersal timing and direction, the issue of when humans first became cognitively and culturally able to extend their climatic tolerance beyond their physiological limits remains very difficult to decipher.

Here, we address the more restricted issue of when during the history of *Homo* the limits of climatic tolerance expanded and which species were involved. We do not specifically address the cultural and social adaptations that might underlie such tolerance but rather consider the implications of our findings for the timing of such adaptations. We model the evolution of climatic tolerance (i.e. niche) limits in the *Homo* genus by associating paleoclimatic values with fossil occurrences in the archaeological record. Specifically, we test the hypothesis that *H. sapiens* developed greater climatic tolerance relative to *H. heidelbergensis* and *H. neanderthalensis* against the alternative that the exploration of climates outside natural physiological limits had already begun with the earliest of these species.

To test this hypothesis, we estimated the rate of change of climatic tolerance limits across the human phylogenetic tree and searched for possible shifts in the rate. We apply a method which allows us to compute the rate of evolution of climatic niche limits at each branch in the tree. In the present context, shifts in the rate of evolution of climatic tolerance that accrue to the clade including the Happisburgh/Pakefield hominins, *H. heidelbergensis*, plus *H. neanderthalensis*, and *H. sapiens* (modern *Homo* species, MHS, hereafter) would indicate these hominins were the first to acquire the capacity to develop cold climate-related technological skills and cultural adaptations. Conversely, if either no rate shift occurs or the rate shift coincides with different clades (e.g. early *Homo* species, EHS, hereafter), the colonization of Northern habitats would not be indicative of any sudden increase in the ability to face environmental harshness.

The human fossil data set we used includes 2,597 occurrences of hominid remains and artifacts associated with 727 archaeological sites. The time range of our record spans from the first occurrence of Australopiths in East Africa dated to some 4.2 Ma to the definitive advent of *H. sapiens* in Eurasia almost coincident with the demise of *H. neanderthalensis* dated at 0.040 Ma (see Data S1, Raia et al., 2020). Such a wide range of hominin taxa provides a thorough phylogenetic context for the analyses.

Deriving spatiotemporally detailed climate data for the past requires dynamic climate modeling, but the timescales for human evolution exceed the possibilities of direct model simulation by several orders of magnitude. To circumvent this limitation, we combine direct simulation using a computationally efficient, intermediate complexity Earth system model, the Planet Simulator–Grid-Enabled Integrated Earth system model (PLASIM-GENIE), with statistical modeling, to create PALEO-PGEM, a paleoclimate emulator, capable of performing multi-million year simulations forced by observationally derived proxy time series for ice sheet state, CO_2 concentration, and orbital forcing (Holden et al., 2016, 2019). To model the realized climatic niche evolution, we applied phylogenetic ridge regression ("RRphylo", Castiglione et al., 2018). "RRphylo" allows us to compute evolutionary rates for each branch of the phylogeny and to estimate the ancestral phenotypes (Raia et al., 2018; Melchionna et al., 2020b; Baab, 2018). Here, the "phenotype" comprises climatic tolerance limits.

By using past annual maxima and minima for temperature, precipitation, and net primary productivity from PALEO-PGEM, we reconstructed and projected onto the geographical space the climatic niche limits

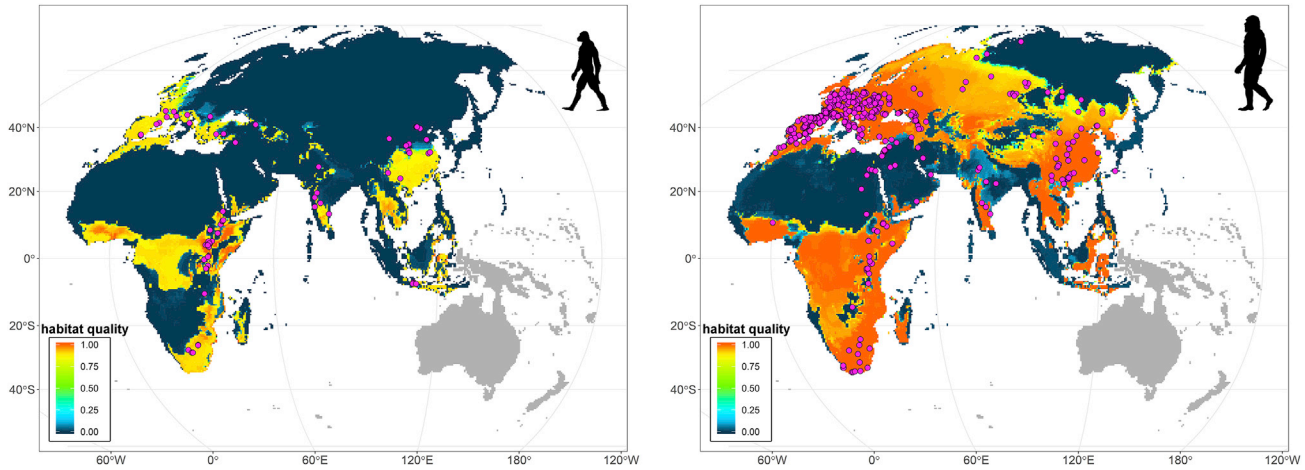

Figure 1. Habitat Quality Map for Early *Homo* Species (EHS, Left) and Modern *Homo* Species (MHS, Right)

The maps show the quality of the habitats potentially suitable for occupation by the common ancestors of EHS and MHS, respectively. Quality varies from little (blue) to highly suitable (red) areas. The fossil occurrences of EHS (*H. habilis*, *H. ergaster*, and *H. erectus*) and MHS (*H. heidelbergensis*, *H. neanderthalensis*, and *H. sapiens*) are superimposed on each map (pink dots). See also Figure S1 and Table S1.

corresponding to the ancestral species distributions (the nodes in the tree) in our fossil database. Using "RRphylo", we were then able to infer climatic niche tolerance limits (Quintero and Wiens, 2013) for each node in the tree and to assess whether the rate of climatic niche evolution shows any shift (i.e. acceleration or deceleration) consistent with our starting hypothesis, while accounting for the effect of shared inheritance. We accounted for phylogenetic uncertainty by perturbing the tree node ages and the tree topology randomly one hundred times. By incorporating phylogenetic uncertainty in this way, we were able to define an overall "habitat quality" (HQ) metric, representing the number of times (out of 100 repetitions) a geographic cell was found habitable (i.e. fell within climatic tolerance limits) for a given ancestor in the tree.

RESULTS

The Association between the Distribution of Fossil Species and Habitat Quality

We used the area under the curve (AUC) metric to measure the association between HQ and the location of fossil occurrences. At AUC = 1, the association would be perfect. AUC = 0 would indicate perfect inverse relation, whereas AUC ~ 0.5 indicates random association. We found that despite the enormous geographic variation in both the preservation potential and the intensity of paleontological sampling (Carotenuto et al., 2010), there is a strong association between the geographic position of archaeological remains and the inferred suitability of the environmental conditions, for both EHS (AUC = 0.80, Figure 1 left, AUC after subsampling the most abundant species = 0.71) and MHS (AUC = 0.81, Figure 1 right, AUC after subsampling the most abundant species = 0.82). This strong association remains valid for all nodes in the hominin tree (Figures S1 and S2, Tables 1 and S2) and suggests that climatic variation in time and space strongly controlled the geographic ranges of our ancestors. Excluding extreme climatic values (i.e. climatic records beyond the 90th percentile of the individual variable distributions) in order to mitigate the effect of potential errors in the paleoclimate emulator, the AUC value for EHS decreased to 0.68, whereas it increased to as much as 0.82 for MHS (Table S3, Figure S3). We repeated this test by randomly placing species fossil occurrences throughout their biogeographical domain (Table S4, Figure S4) to simulate a scenario of no association between the archaeological record and HQ. Under this simulation, the AUC values drop toward 0.5, which indicate non-significant association between the two variables (EHS AUC = 0.56; 95%, confidence interval: 0.52–0.61; MHS AUC = 0.58, confidence interval: 0.56–0.60). This finding reinforces the notion that the geographic position of archaeological sites is a non-random process guided by climatic variability.

Rates of Hominin Climatic Niche Limit Evolution

We found that the clade identified by *H. heidelbergensis*, *H. neanderthalensis*, and *H. sapiens* and their common ancestor experienced a significant evolutionary rate shift toward wider climatic tolerance (Figure 2). The rate shift does not depend on the specific phylogenetic hypothesis (tree topology) assumed,

Species	Shift	Node with Two Species	Node with Three Species	*H. heidelbergensis*	*H. neanderthalensis*	*H. sapiens*
H. heidelbergensis	86	23	63	/	75	74
H. neanderthalensis	85	22	63	74	/	74
H. sapiens	86	23	63	75	74	/

Table 1. Percentage of Significant Rate Shifts in Niche Width Calculated through Phylogenetic Reshuffling

The table lists the percentage of significant shifts that occurred at nodes with two or three species, as well as the occurrence of each of the three *Homo* species in each significant shift.

neither does it depend on the selection of species we used. Randomly changing the tree node ages (to account for dating uncertainty) and species positions in the hominin tree (to account for phylogenetic uncertainty) 100 times, the shift appears for this clade 95 times (Table 1). Subsampling the most abundant species (randomly selecting no more than 100 fossil occurrences per species) to account for sampling differences between species, the shift appears 91 times out of a hundred. We also repeated the phylogenetic reshuffling randomly removing one species at once. Under this latter design, the MHS shift occurs 63 times out of 100, and 23 additional times the shift involves two, rather than three, MHS species. Individually, *H. sapiens* and *H. heidelbergensis* appear in 86 rate shifts, *H. neanderthalensis* in 85, and no shift appears outside the MHS clade, demonstrating that the rate shift pertains to these species only and is not guided preferentially by any of the three (Table 1).

DISCUSSION

The estimated values of realized climatic niche limits at nodes in the hominin phylogeny suggest that the rate shift in the climatic niche limits for the MHS clade was not an exclusively biological process. At the root of the hominin tree (node 11, Table S1), the predicted range in annual temperatures spans from 20°C (coldest quarter of the year) to 29.9°C (warmest quarter) and in mean rainfall from 12 mm (driest quarter) to 512 mm (wettest quarter). This is entirely consistent with today's African savannah environment (Hijmans et al., 2005). At the node subtending the pair *H. ergaster* plus *H. erectus* (which is the first hominin to disperse over Southern Eurasia), the corresponding figures are 0.7°C–31.9°C for temperature range and from 4.8 mm to 1080 mm for precipitation range. These estimates are reasonable considering both the range expansion into temperate regions and the colonization of warm and humid environments (Indonesia) by *H. erectus* (Carotenuto et al., 2016; Joordens et al., 2015; Rizal et al., 2019). Yet, at the common ancestor to the three MHS, the estimates for annual temperature extremes span from minus 21.1°C to plus 31.4°C and for annual precipitation from 0.7 mm to 905 mm. Although the common ancestor to MHS was an African species which probably never experienced these extreme climates (Profico et al., 2016), the values agree qualitatively with the notion that a sudden widening of climatic niche limits occured with the advent of this ancestor, whose offspring lived after the onset of fully glacial Pleistocene conditions (Churchill, 1998). The massive increase in the estimated range of thermal conditions suitable for the MHS clade taxa (marked by a 20°C decrease in minimum temperature of the coldest season of the year as compared to the hominin tree root, Figures 3 and S5) does not depend on the phylogenetic hypothesis we applied and surpasses what is expected by a random process of increased phenotypic variance over time (namely the Brownian motion model of evolution, see Supplemental Information for full explanation). Using 100 different tree topologies and branch lengths to account for phylogenetic uncertainty, we found a significant trend in the temperature of the coldest season realized by hominins 97 times (Figure 3), whereas no trend was found in the maximum temperatures of the warmest season. We found that in African species and ancestors, the average temperature of the coldest quarter of the year was no less than 9.4°C, meaning that the winter chill is unlikely to have been a problem for them (Table S5). In contrast, within the range of temperatures experienced by *H. heidelbergensis*, the coldest quarter of the year was as cold as −12.3°C, suggesting specific technological and cultural adaptations were needed to fend off the risk of hypothermia and to live in the highly seasonal, cold northern environments (Ulijaszek and Strickland, 1993; Ellison et al., 2005; Gilligan, 2007; Rivals et al., 2009; El Zaatari et al., 2016). These adaptations may have included fitted clothing (Amanzougaghene et al., 2019), thrown spears (Lenoir and Villa, 2006) or adhesives (Cârciumaru et al., 2012), and enhanced healthcare practices (Spikins et al., 2019).

For some, the process of cultural niche construction (Laland et al., 2001; Laland and O'Brien, 2012) through which human cultural traits have changed the human adaptive niche and in turn selective pressures and

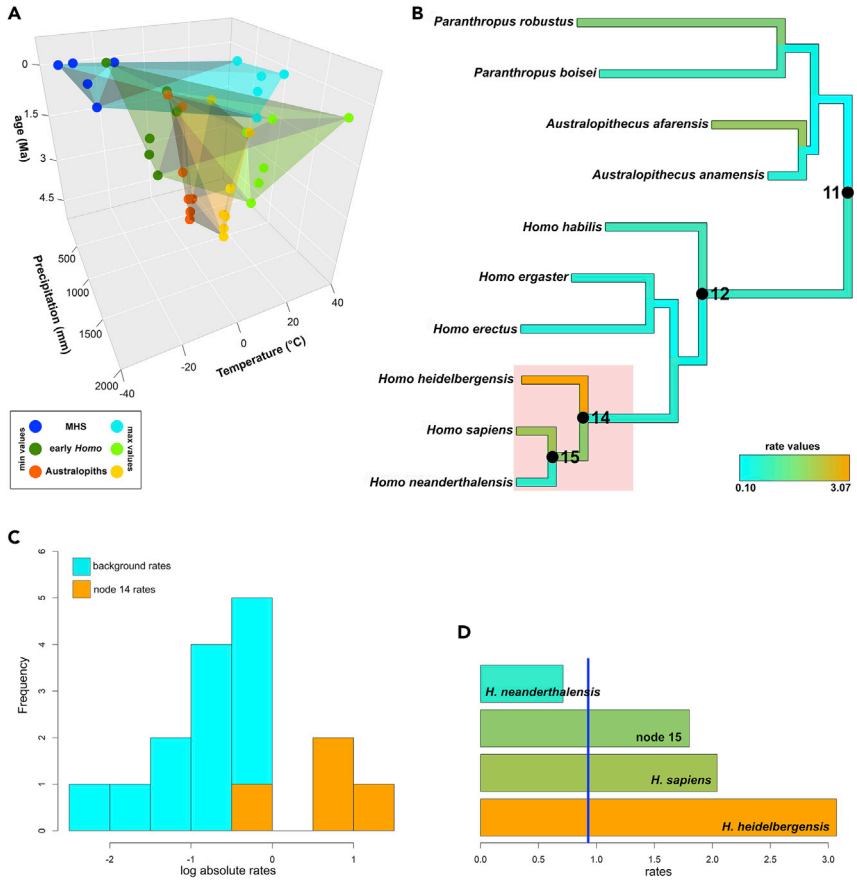

Figure 2. Climatic Niche Evolution in Hominins

(A) Three-dimensional plot of the climatic niche space occupied by the hominin clades through time.

(B) The hominin tree used in this study. The branch colors are proportional to the multivariate rate of climatic niche evolution for each branch in the tree. At the MHS common ancestor (14), an acceleration in the rate of evolution in climatic tolerance limits occurs (shaded area). The common ancestor to all species within *Homo* is indicated by node 12.

(C) The distribution of the rates of niche evolution for the MHS clade (orange) compared to the rest of the branches in the tree (light blue).

(D) The individual rates of niche evolution for the tree branches forming the MHS clade. The average rate for the entire tree is indicated by the vertical blue line. MHS = modern *Homo* species, EHS = *Homo* species exclusive of MHS, Australopiths = species in the genus *Paranthropus* and *Australopithecus*.

ecological inheritance (Odling-Smee and Laland, 2011) traces back to the very emergence of the genus *Homo* at some 2.5 million years ago (Antón and Snodgrass, 2012; Antón et al., 2014). At that time, increasing dependence on stone artifact production and social learning (Hiscock, 2014) and on collaboration (Fuentes et al., 2010; Fuentes, 2015) may have been particularly influential in allowing hominins to not only escape their biological constraints but also actively change the environmental and ecological niches of other species (Low et al., 2019). The occasional use of fire has similarly deep roots in human history (Gowlett, 2016; Organ et al., 2011; Pruetz and Herzog, 2017). Yet, the habitual use of fire (Shimelmitz et al., 2014) and the ability to work hide, wood and ivory (d'Errico and Henshilwood, 2007; Thieme, 1997) is attested at a much later date, during the Middle Stone Age (d'Errico, 2003) and attached to MHS only. Brain asymmetry and right handiness, usually linked with advanced cognitive skills (Crow, 1993; Xiang et al., 2019; Melchionna et al., 2020a), similarly characterize MHS (Frayer et al., 2012; Lozano et al., 2009; Poza-Rey et al., 2017). In contrast to MHS, EHS either did not venture outside Africa or went across Eurasia longitudinally. *Homo erectus* spread across Africa and Eurasia up to Java at some 1.7 Ma but never settled north of the Mediterranean area or southeast China (Carotenuto et al., 2016). From the appearance of *H. heidelbergensis* onward, northern, presumably colder habitats were no longer completely uninhabitable.

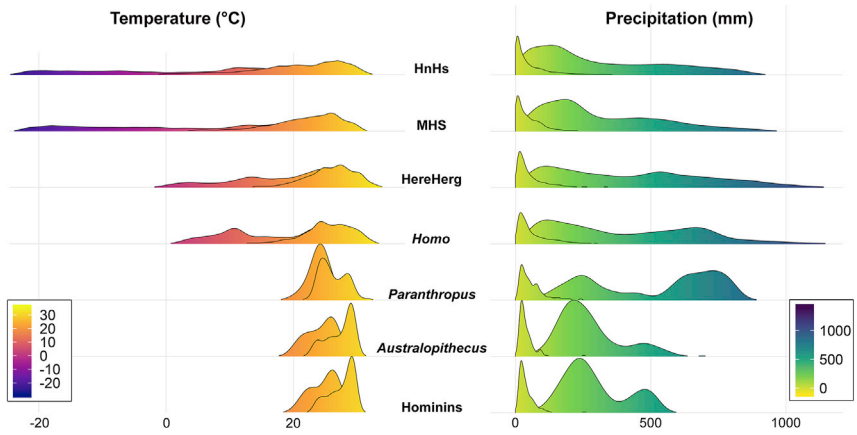

Figure 3. Estimated Temperature and Precipitation Ranges at Several Nodes in the Human Phylogenetic Tree

The individual rows represent the density distribution of minimum and maximum temperature and precipitation, respectively, collapsed together. HnHs = common ancestor to *H. neanderthalensis* and *H. sapiens*, MHS = common ancestor to *H. heidelbergensis*, *H. neanderthalensis*, and *H. sapiens* HereHerg = common ancestor to *H. erectus* and *H. ergaster*, *Homo* = common ancestor to *Homo* species, *Paranthropus* = common ancestor to all *Paranthropus* species, *Australopithecus* = common ancestor to all *Australopithecus* species, Hominins = common ancestor to hominins.

The jump in the rates of evolution in climatic niche width (driven by a sudden increase in tolerance to the cold, Figure 3) had enormous consequence in terms of geographic range. By modeling climatic niche limits according to a random walk with constant variance process (i.e. the Brownian motion model of evolution, BM) and assuming as habitable all geographic cells with HQ >0.25, the rate shift accounts for a twofold increase in viable geographic range at the ancestor of MHS (node 14 in the tree) for a net gain of some 30×10^6 km^2 (roughly the land surface of the African continent). At node 15, the ancestor of *H. sapiens* and *H. neanderthalensis*, the habitable area becomes nearly three times larger than expected under BM, corresponding to a geographic extension of some 50×10^6 km^2. This massive increase in habitable area mostly represents expansion into northern latitudes, testifying to the importance of the rate shift in the colonization of Eurasia (Figure S5).

Although there is consistent evidence that *Homo* species may have exchanged genes with positive fitness consequences in cold environments by means of genetic introgression, this evidence is limited to the last 40 kya and invariably pertains to local *Homo sapiens* populations (Huerta-Sánchez et al., 2014; Sánchez-Quinto and Lalueza-Fox, 2015), meaning it occurs much later than the rate shift, and after the actual colonization of northern territories.

Although the real consequences of any individual cultural or technological adaptation introduced by MHS will almost certainly be a matter for debate for some time, our results indicate that these hominins were able to overcome the challenges imposed by life in northern habitats by a non-biological process, suggesting that behavioral modernity, interpreted as the capacity to use technology and culture to overcome the constraints imposed by natural climate variability on the geographic distribution, is not limited to *H.* sapiens.

Limitations of the Study

The very concept of niche construction in *Homo* implies cultural advancements (fitted clothing manufacture, intentional fire, the production of tools made of perishable material such as bone, hide and wood) and improved social connections and skills that leave little to no archaeological evidence (Riede, 2019). Rather than focusing on such scarce evidence, we therefore focused on one of the major consequences of these cultural advances, that is, the occupation of areas and climates outside the physiological niche limits of humans. A limitation of our findings is that the precise connection between the expansion of the climatic niche limits and advancements in material culture cannot easily be determined. Still, it relies on paleoclimate modeling that necessarily comes with uncertainty around the estimates. Nevertheless, our study confidently demonstrates the importance of cultural niche construction in the evolution of *Homo* and how the sudden evolution of such niche construction abilities shaped the geography of our own lineage in the deep past.

Resource Availability

Lead Contact

Further information and requests for resources should be directed to Pasquale Raia (pasquale.raia@unina.it).

Materials Availability

This study did not generate any new material.

Data and Code Availability

The human fossil record and phylogenetic tree of hominins are available as supplemental data files. The functions used in this study are freely available as parts of the package RRphylo. Environmental niche limits (climatic variables) for each hominin species to generate estimates at the tree nodes (ancestors) are available in Table S1.

METHODS

All methods can be found in the accompanying Transparent Methods supplemental file.

SUPPLEMENTAL INFORMATION

Supplemental Information can be found online at https://doi.org/10.1016/j.isci.2020.101693.

ACKNOWLEDGMENTS

We are grateful to Fabio di Vincenzo and Giorgio Manzi for critical discussion about the main findings presented here.

AUTHOR CONTRIBUTIONS

P.R., A.M., M.M., and M.D.F. conceived the study. A.M., M.M., M.Mod., T.R., A.P., N.E., and P.H. produced and collected the data. A.M., M.M., M.D.F., S.C., and C.S. performed the analyses. P.O.H., F.C., L.M., L.R., J.A.D.F., T.R., A.P., N.E., and P.H. contributed in critique of analyses and interpretation. P.S. contributed in discussion of cultural and social contexts. All the authors contributed to writing.

DECLARATION OF INTERESTS

The authors declare no conflict of interests.

Received: August 3, 2020
Revised: September 3, 2020
Accepted: October 13, 2020
Published: November 20, 2020

REFERENCES

Antón, S.C., and Snodgrass, J.J. (2012). Origins and evolution of genus homo: new perspectives. Curr. Anthropol. *53*, S479–S496.

Antón, S.C., Potts, R., and Aiello, L.C. (2014). Human evolution. Evolution of early homo: an integrated biological perspective. Science *345*, 1236828.

Amanzougaghene, N., Fenollar, F., Raoult, D., and Mediannikov, O. (2019). Where are we with human lice? A review of the current state of knowledge. Front. Cell. Infect. Microbiol. *9*, 213.

Baab, K.L. (2018). Evolvability and craniofacial diversification in genus Homo. Evolution *72*, 2781–2791.

Banks, W.E., d'Errico, F., Dibble, H.L., Krishtalka, L., West, D., Olszewski, D., Townsend Peterson, A., Anderson, D.G., Gillam, G.C., Montet-White, A., et al. (2006). Eco-cultural niche modeling: new tools for reconstructing the geography and ecology of past human populations. Palaeoanthropology *4*, 68–83.

Banks, W.E., d'Errico, F., Peterson, A.T., Vanhaeren, M., Kageyama, M., Sepulchre, P., Ramstein, G., Jost, A., and Lunt, D. (2008). Human ecological niches and ranges during the lgm in Europe derived from an application of eco-cultural niche modeling. J. Archaeol. Sci. *35*, 481–491.

Banks, W.E., Aubry, T., d'Errico, F., Zilhão, J., Lira-Noriega, A., and Townsend Peterson, A. (2011). Eco-cultural niches of the badegoulian: unraveling links between cultural adaptation and ecology during the last glacial maximum in France. J. Anthr. Archaeol. *30*, 359–374.

Banks, W.E., d'Errico, F., and Zilhão, J. (2013). Human–climate interaction during the early upper paleolithic: testing the hypothesis of an adaptive shift between the proto-aurignacian and the early aurignacian. J. Hum. Evol. *64*, 39–55.

Benito, B.M., Svenning, J.-C., Kellberg-Nielsen, T., Riede, F., Gil-Romera, G., Mailund, T., Kjaergaard, P.C., and Sandel, B.S. (2017). The ecological niche and distribution of neanderthals during the last interglacial. J. Biogeogr. *44*, 51–61.

Boivin, N.L., Zeder, M.A., Fuller, D.Q., Crowther, A., Larson, G., Erlandson, J.M., Denham, T., and Petraglia, M.D. (2016). Ecological consequences of human niche construction: examining long-term anthropogenic shaping of global species distributions. Proc. Natl. Acad. Sci. U S A *113*, 6388–6396.

Cârciumaru, M., Ion, R.-M., Niţu, E.-C., and Ştefănescu, R. (2012). New evidence of adhesive as hafting material on middle and upper palaeolithic artefacts from Gura Cheii-Râşnov Cave (Romania). J. Archaeol. Sci. *39*, 1942–1950.

Carotenuto, F., Barbera, C., and Raia, P. (2010). Occupancy, range size, and phylogeny in Eurasian Pliocene to Recent large mammals. Paleobiology *36*, 399–414.

Carotenuto, F., Tsikaridze, N., Rook, L., Lordkipanidze, D., Longo, L., Condemi, S., and Raia, P. (2016). Venturing out safely: the biogeography of Homo erectus dispersal out of Africa. J. Hum. Evol. *95*, 1–12.

Castiglione, S., Tesone, G., Piccolo, M., Melchionna, M., Mondanaro, A., Serio, C., Di Febbraro, M., and Raia, P. (2018). A new method for testing evolutionary rate variation and shifts in phenotypic evolution. Methods Ecol. Evol. *9*, 974–983.

Churchill, S.E. (1998). Cold adaptation, heterochrony, and Neandertals. Evol. Anthropol. *7*, 46–60.

Crow, T.J. (1993). Sexual selection, Machiavellian intelligence, and the origins of psychosis. Lancet *342*, 594–598.

d'Errico, F. (2003). The invisible frontier. A multiple species model for the origin of behavioral modernity. Evol. Anthropol. *12*, 188–202.

d'Errico, F., and Henshilwood, C.S. (2007). Additional evidence for bone technology in the southern African middle stone age. J. Hum. Evol. *52*, 142–163.

Dunbar, R.I.M., Gamble, C., and Gowlett, J.A.J. (2014). Lucy to Language (Oxford University Press).

El Zaatari, S., Grine, F.E., Ungar, P.S., and Hublin, J.-J. (2016). Neandertal versus modern human dietary responses to climatic fluctuations. PLoS One *11*, e0153277.

Ellison, P.T., Valeggia, C.R., and Sherry, D.S. (2005). Human birth seasonality. In Seasonality in Primates: Studies of Living and Extinct Human and Non-human Primates, D.K. Brockman and C.P. van Schaik, eds. (Cambridge University Press), p. 379.

Frayer, D.W., Lozano, M., Bermúdez de Castro, J.M., Carbonell, E., Arsuaga, J.-L., Radovčić, J., Fiore, I., and Bondioli, L. (2012). More than 500,000 years of right-handedness in Europe. Laterality *17*, 51–69.

Fuentes, A. (2015). Integrative anthropology and the human niche: toward a contemporary approach to human evolution. Am. Anthropol. *117*, 302–315.

Fuentes, A., Wyczalkowski, M.A., and MacKinnon, K.C. (2010). Niche construction through cooperation: a nonlinear dynamics contribution to modeling facets of the evolutionary history in the genus Homo. Curr. Anthropol. *51*, 435–444.

Gilligan, I. (2007). Neanderthal extinction and modern human behaviour: the role of climate change and clothing. World Archaeol. *39*, 499–514.

Gilligan, I. (2010). The prehistoric development of clothing: archaeological implications of a thermal model. J. Archaeol. Method Theor. *17*, 15–80.

Gowlett, J.A.J. (2016). The discovery of fire by humans: a long and convoluted process. Philos. Trans. R. Soc. B *371*, 20150164.

Harmand, S., Lewis, J.E., Feibel, C.S., Lepre, C.J., Prat, S., Lenoble, A., Boës, X., Quinn, R.L., Brenet, M., Arroyo, A., et al. (2015). 3.3-million-year-old stone tools from lomekwi 3, West Turkana, Kenya. Nature *521*, 310–315.

Henshilwood, C.S., d'Errico, F., Yates, R., Jacobs, Z., Tribolo, C., Duller, G.A.T., Mercier, N., Sealy, J.C., Valladas, H., Watts, I., and Wintle, A.G. (2002). Emergence of modern human behavior: middle stone age engravings from South Africa. Science *295*, 1278–1280.

Hijmans, R.J., Cameron, S.E., Parra, J.L., Jones, P.G., and Jarvis, A. (2005). Very high resolution interpolated climate surfaces for global land areas. Int. J. Climatol. *25*, 1965–1978.

Hiscock, P. (2013). 5 Early Old World Migrations of Homo sapiens: Archaeology (Blackwell Publishing Ltd).

Hiscock, P. (2014). Learning in lithic landscapes: a reconsideration of the hominid 'toolmaking' niche. Biol. Theory *9*, 27–41.

Holden, P.B., Edwards, N.R., Fraedrich, K., Kirk, E., Lunkeit, F., and Zhu, X. (2016). PLASIM–GENIE v1. 0: a new intermediate complexity AOGCM. Geosci. Model Dev. *9*, 3347–3361.

Holden, P.B., Edwards, N.R., Rangel, T.F., Pereira, E.B., Tran, G.T., and Wilkinson, R.D. (2019). PALEO-PGEM v1. 0: a statistical emulator of Pliocene–Pleistocene climate. Geosci. Model Dev. *12*, 5137–5155.

Hosfield, R. (2016). Walking in a winter wonderland? Strategies for early and middle Pleistocene survival in midlatitude Europe. Curr. Anthropol. *57*, 653–682.

Huerta-Sánchez, E., Jin, X., Asan, Bianba, Z., Peter, B.M., Vinckenbosch, N., Liang, Y., Yi, X., He, M., Somel, M., et al. (2014). Altitude adaptation in Tibetans caused by introgression of Denisovan-like DNA. Nature *512*, 194–197.

Joordens, J.C.A., d'Errico, F., Wesselingh, F.P., Munro, S., de Vos, J., Wallinga, J., Ankjærgaard, C., Reimann, T., Wijbrans, J.R., Kuiper, K.F., et al. (2015). Homo erectus at Trinil on Java used shells for tool production and engraving. Nature *518*, 228–231.

Kittler, R., Kayser, M., and Stoneking, M. (2003). Molecular evolution of Pediculus humanus and the origin of clothing. Curr. Biol. *13*, 1414–1417.

Laland, K.N., Odling Smee, J., and Feldman, M.W. (2001). Cultural niche construction and human evolution. J. Evol. Biol. *14*, 22–33.

Laland, K.N., and O'Brien, M.J. (2012). Cultural niche construction: an introduction. Biol. Theory *6*, 191–202.

Lee-Thorp, J.A., Sponheimer, M., Passey, B.H., de Ruiter, D.J., and Cerling, T.E. (2010). Stable isotopes in fossil hominin tooth enamel suggest a fundamental dietary shift in the Pliocene. Philos. Trans. R. Soc. B *365*, 3389–3396.

Lenoir, M., and Villa, P. (2006). Hunting weapons of the middle stone age and the middle palaeolithic: spear points from Sibudu, rose cottage and Bouheben. South. Afr. Humanit. *18*, 89–122.

Lordkipanidze, D., Jashashvili, T., Vekua, A., de León, M.S.P., Zollikofer, C.P.E., Rightmire, G.P., Pontzer, H., Ferring, R., Oms, O., Tappen, M., et al. (2007). Postcranial evidence from early Homo from Dmanisi, Georgia. Nature *449*, 305–310.

Low, F.M., Gluckman, P.D., and Hanson, M.A. (2019). Niche modification, human cultural evolution and the anthropocene. Trends Ecol. Evol. *34*, 883–885.

Lozano, M., Mosquera, M., de Castro, J.-M.B., Arsuaga, J.-L., and Carbonell, E. (2009). Right handedness of Homo heidelbergensis from Sima de los Huesos (Atapuerca, Spain) 500,000 years ago. Evol. Hum. Behav. *30*, 369–376.

Martin, J.S., Ringen, E.J., Duda, P., and Jaeggi, A.V. (2020). Harsh environments promote alloparental care across human societies. Proc. R. Soc. B *287*, 20200758.

Melchionna, M., Profico, A., Castiglione, S., Sansalone, G., Serio, C., Mondanaro, A., Di Febbraro, M., Rook, L., Pandolfi, L., Di Vincenzo, F., et al. (2020a). From smart apes to human brain boxes. A uniquely derived brain shape in late hominins clade. Front. Earth Sci. *8*, 273.

Melchionna, M., Mondanaro, A., Serio, C., Castiglione, S., Di Febbraro, M., Rook, L., Diniz-Filho, J.A.F., Manzi, G., Profico, A., Sansalone, G., and Raia, P. (2020b). Macroevolutionary trends of brain mass in primates. Biol. J. Linn. Soc. *129*, 14–25.

Nicholson, C.M. (2019). Shifts along a spectrum: a longitudinal study of the western eurasian realized climate niche. Environ. Archaeol. 1–16.

Odling-Smee, J., and Laland, K.N. (2011). Ecological inheritance and cultural inheritance: what are they and how do they differ? Biol. Theory *6*, 220–230.

Organ, C., Nunn, C.L., Machanda, Z., and Wrangham, R.W. (2011). Phylogenetic rate shifts in feeding time during the evolution of Homo. Proc. Natl. Acad. Sci. U S A *108*, 14555–14559.

Parfitt, S.A., Ashton, N.M., Lewis, S.G., Abel, R.L., Coope, G.R., Field, M.H., Gale, R., Hoare, P.G., Larkin, N.R., Lewis, M.D., et al. (2010). Early Pleistocene human occupation at the edge of the boreal zone in northwest Europe. Nature *466*, 229–233.

Pearce, E., Shuttleworth, A., Grove, M., and Layton, R. (2014). The costs of being a high latitude hominin. In Lucy to Language: The Benchmark Papers, R.I.M. Dunbar, C. Gamble, and J.A.J. Gowlett, eds. (Oxford University Press), pp. 356–379.

Poza-Rey, E.M., Lozano, M., and Arsuaga, J.-L. (2017). Brain asymmetries and handedness in the specimens from the Sima de los Huesos site (Atapuerca, Spain). Quat. Int. *433*, 32–44.

Profico, A., Di Vincenzo, F., Gagliardi, L., Piperno, M., and Manzi, G. (2016). Filling the gap. Human cranial remains from Gombore II (Melka Kunture, Ethiopia; ca. 850 ka) and the origin of Homo heidelbergensis. J. Anthropol. Sci. *94*, 1–24.

Pruetz, J.D., and Herzog, N.M. (2017). Savanna chimpanzees at Fongoli, Senegal, navigate a fire landscape. Curr. Anthropol. *58*, S337–S350.

Quintero, I., and Wiens, J.J. (2013). What determines the climatic niche width of species? The role of spatial and temporal climatic variation in three vertebrate clades. Glob. Ecol. Biogeogr. *22*, 422–432.

Rae, T.C., Koppe, T., and Stringer, C.B. (2011). The Neanderthal face is not cold adapted. J. Hum. Evol. *60*, 234–239.

Raia, P., Boggioni, M., Carotenuto, F., Castiglione, S., Di Febbraro, M., Di Vincenzo, F., Melchionna, M., Mondanaro, A., Papini, A., Profico, A., et al. (2018). Unexpectedly rapid evolution of mandibular shape in hominins. Sci. Rep. *8*, 1–8.

Raia, P., Mondanaro, A., Melchionna, M., Di Febbraro, M., Diniz-Filho, J.A.F., Rangel, T.F., Holden, P.B., Carotenuto, F., Edwards, N.R., Lima-Ribeiro, M.S., et al. (2020). Past extinctions of Homo species coincided with increased vulnerability to climatic change. One Earth. https://doi.org/10.1016/j.oneear.2020.09.007.

Riede, F. (2019). Niche construction theory and human biocultural evolution. In Handbook of Evolutionary Research in Archaeology, A. Prentiss, ed. (Springer), pp. 337–358.

Rivals, F., Moncel, M.-H., and Patou-Mathis, M. (2009). Seasonality and intra-site variation of neanderthal occupations in the middle palaeolithic locality of payre (ardèche, France) using dental wear analyses. J. Archaeol. Sci. *36*, 1070–1078.

Rizal, Y., Westaway, K.E., Zaim, Y., van den Bergh, G.D., Bettis, E.A., Morwood, M.J., Huffman, O.F., n, R.G.X., Joannes-Boyau, R., Bailey, R.M., et al. (2019). Last appearance of Homo erectus at Ngandong, Java, 117,000–108,000 years ago. Nature *577*, 381–385.

Roberts, P., and Stewart, B.A. (2018). Defining the "generalist specialist" niche for Pleistocene Homo sapiens. Nat. Hum. Behav. *2*, 542–550.

Sánchez-Quinto, F., and Lalueza-Fox, C. (2015). Almost 20 years of Neanderthal palaeogenetics: adaptation, admixture, diversity, demography and extinction. Philos. Trans. R. Soc. B *370*, 20130374.

Shimelmitz, R., Kuhn, S.L., Jelinek, A.J., Ronen, A., Clark, A.E., and Weinstein-Evron, M. (2014). 'Fire at will': the emergence of habitual fire use 350,000 years ago. J. Hum. Evol. *77*, 196–203.

Spikins, P., Needham, A., Wright, B., Dytham, C., Gatta, M., and Hitchens, G. (2019). Living to fight another day: the ecological and evolutionary significance of Neanderthal healthcare. Quat. Sci. Rev. *217*, 98–118.

Thieme, H. (1997). Lower Palaeolithic hunting spears from Germany. Nature *385*, 807–810.

Ulijaszek, S.J., and Strickland, S.S. (1993). Seasonality and Human Ecology (Cambridge University Press).

Villmoare, B., Kimbel, W.H., Seyoum, C., Campisano, C.J., DiMaggio, E.N., Rowan, J., Braun, D.R., Arrowsmith, J.R., and Reed, K.E. (2015). Paleoanthropology. Early Homo at 2.8 Ma from Ledi-Geraru, Afar, Ethiopia. Science *347*, 1352–1355.

White, T.D., Asfaw, B., Beyene, Y., Haile-Selassie, Y., Lovejoy, C.O., Suwa, G., and WoldeGabriel, G. (2009). Ardipithecus ramidus and the paleobiology of early hominids. Science *326*, 64–86.

Wroe, S., Parr, W.C.H., Ledogar, J.A., Bourke, J., Evans, S.P., Fiorenza, L., Benazzi, S., Hublin, J.-J., Stringer, C., Kullmer, O., et al. (2018). Computer simulations show that Neanderthal facial morphology represents adaptation to cold and high energy demands, but not heavy biting. Proc. R. Soc. B *285*, 20180085.

Xiang, L., Crow, T., and Roberts, N. (2019). Cerebral torque is human specific and unrelated to brain size. Brain Struct. Funct. *224*, 1141–1150.

Xu, C., Kohler, T.A., Lenton, T.M., Svenning, J.C., and Scheffer, M. (2020). Future of the human climate niche. Proc. Natl. Acad. Sci. U S A *117*, 11350–11355.

iScience, Volume *23*

Supplemental Information

A Major Change in Rate of Climate Niche Envelope Evolution during Hominid History

Alessandro Mondanaro, Marina Melchionna, Mirko Di Febbraro, Silvia Castiglione, Philip B. Holden, Neil R. Edwards, Francesco Carotenuto, Luigi Maiorano, Maria Modafferi, Carmela Serio, Josè A.F. Diniz-Filho, Thiago Rangel, Lorenzo Rook, Paul O'Higgins, Penny Spikins, Antonio Profico, and Pasquale Raia

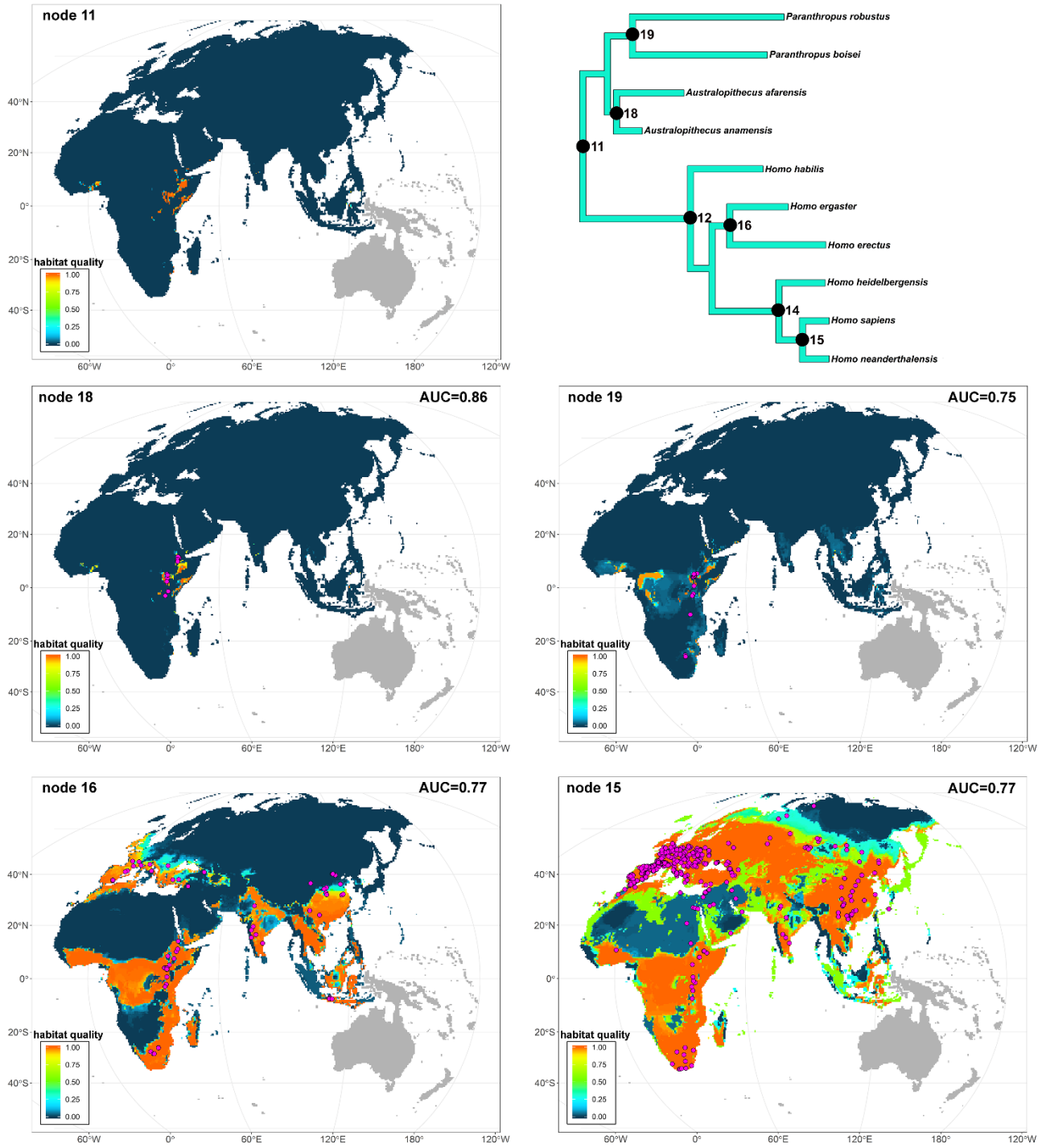

Figure S1. Maps of fossil locality distribution and habitat quality at specific nodes in the hominin tree. Related to Figures 1 and 2.

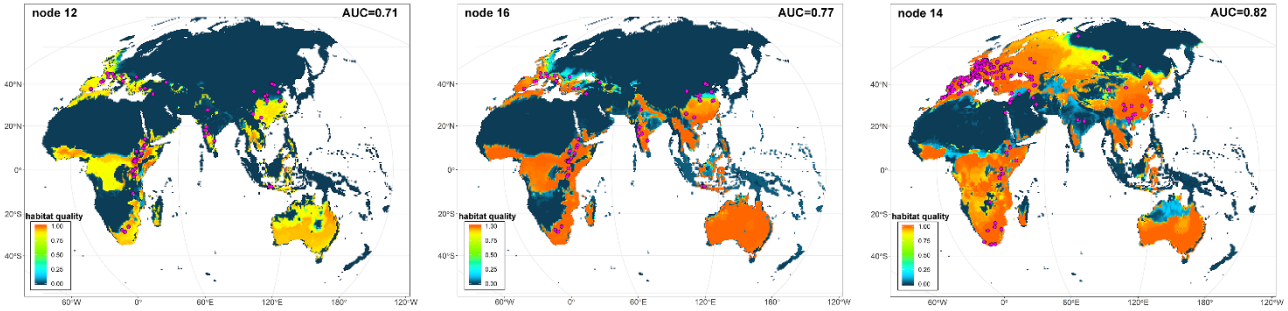

Figure S2. Maps of fossil locality distribution and habitat quality at specific nodes in the hominin tree, after setting the maximum number of fossil localities per species at 100 for the ancestor to all *Homo* species (node 12, left), early *Homo* (node 16, middle) and MHS (node 14, right). Related to Figures 1 and 2.

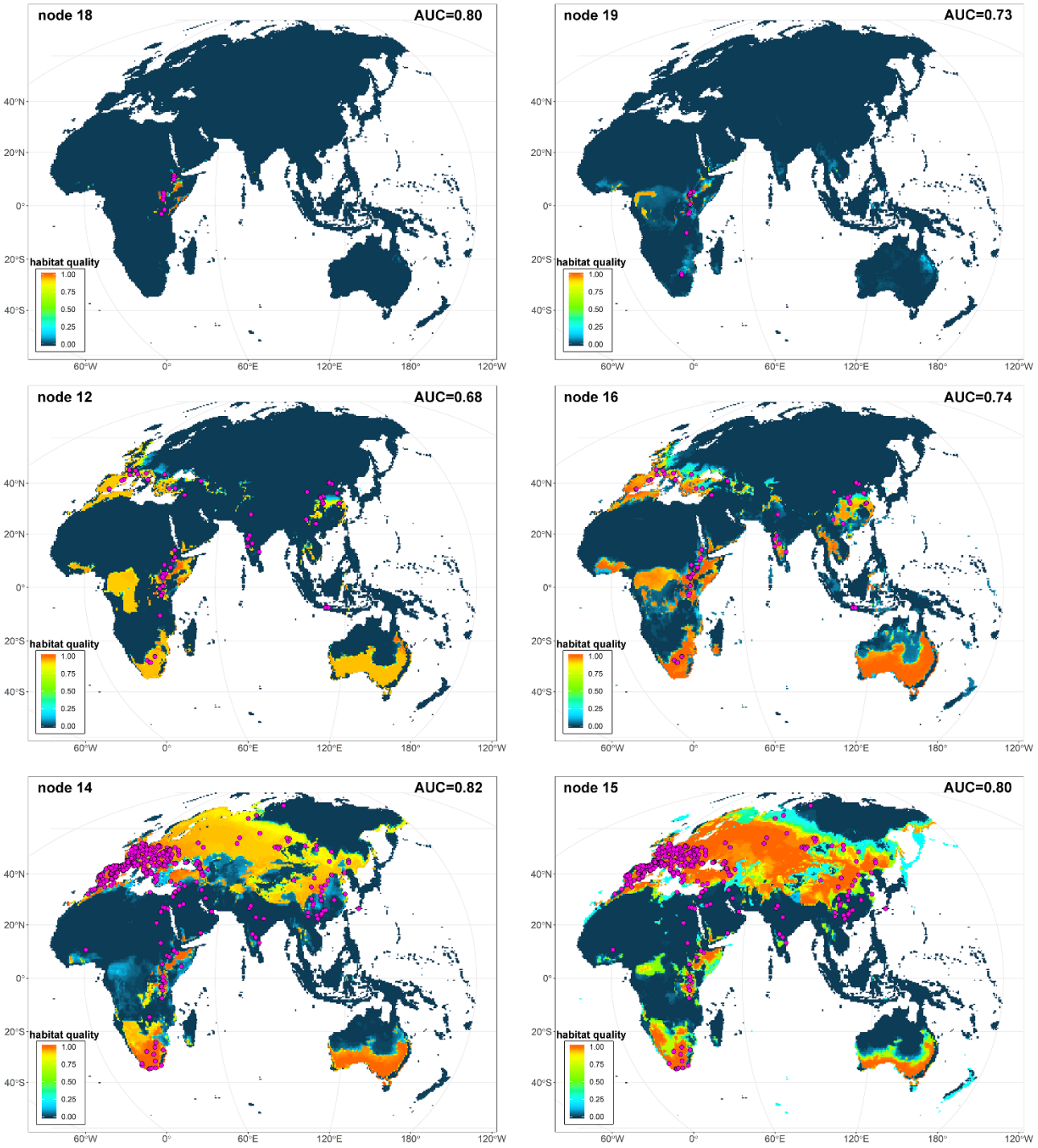

Figure S3. Maps of fossil locality distribution and habitat quality at specific nodes in the hominin tree, after excluding the first decile of the distribution of paleoclimatic estimates. The node numbers correspond to the tree in Figure S1. Related to Figures 1 and 2.

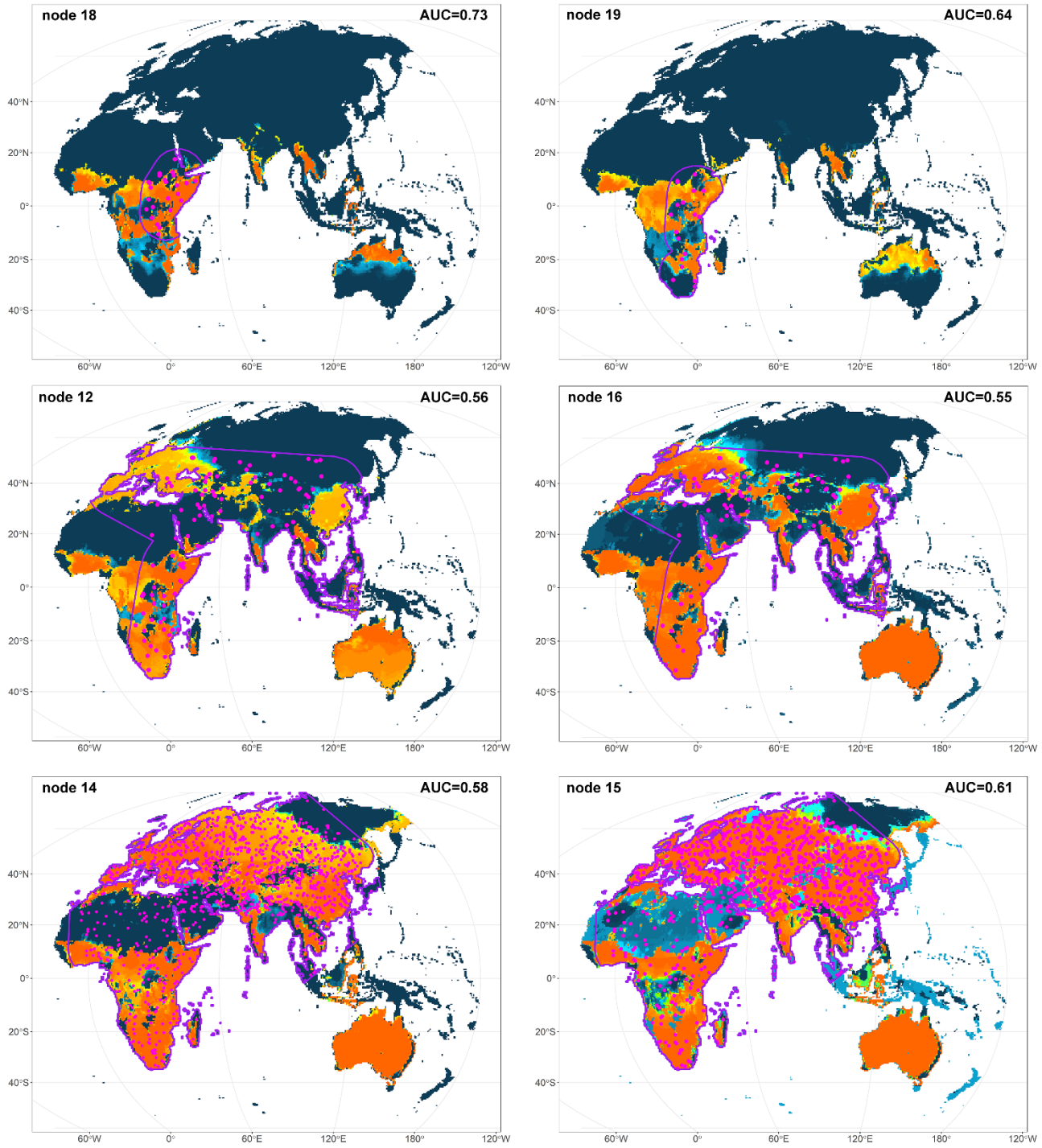

Figure S4. Maps showing randomly placed fossil localities and habitat quality at specific nodes in the hominin tree. Related to Figures 1 and 2.

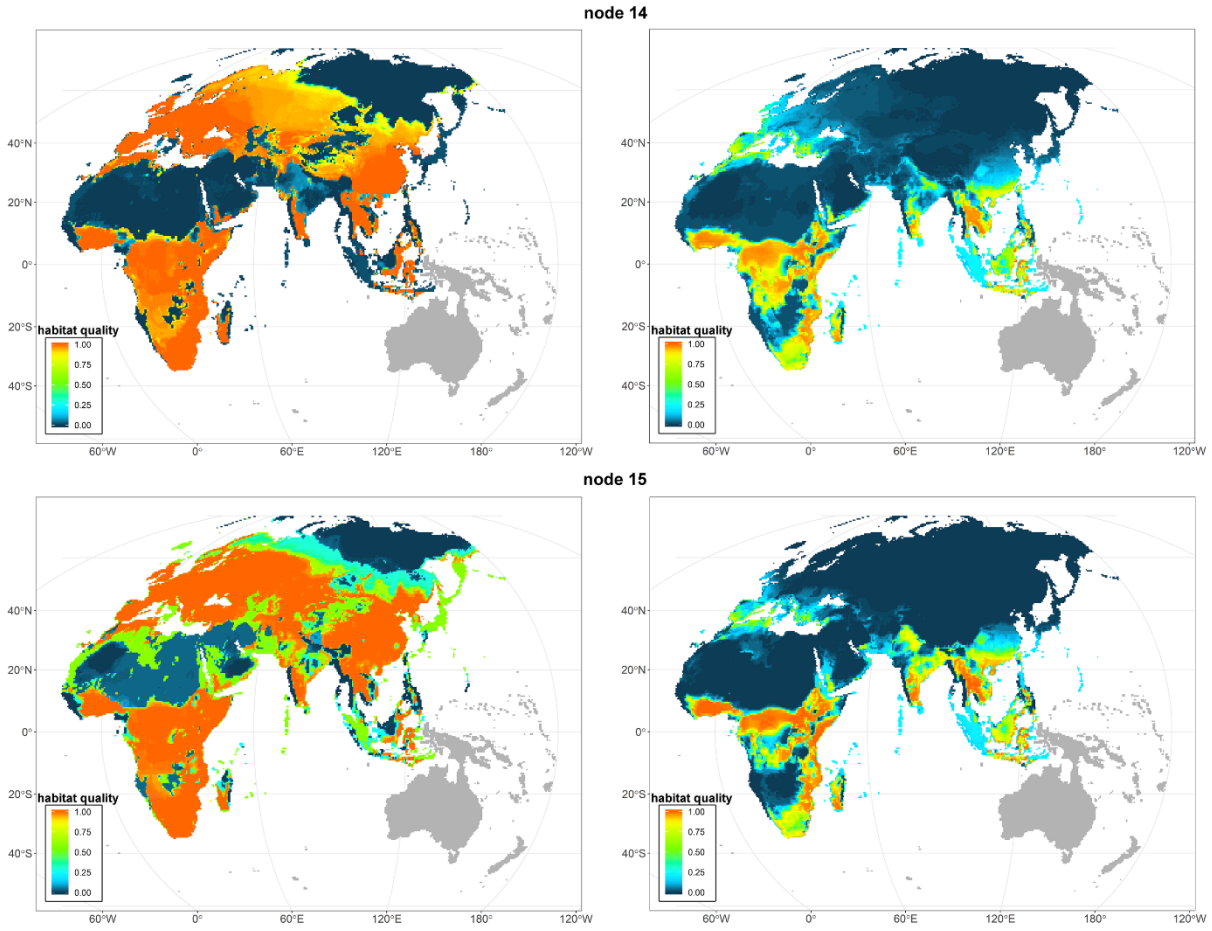

Figure S5. Maps of habitat quality estimated for the ancestors of MHS (node 14 in the tree) and the ancestor of *H. sapiens* plus *H. neanderthalensis* (node 15). Related to Figures 1 and 2.

A

Species	minPrec (mm)	minTemp (°C)	Min NPP	maxPrec (mm)	maxTemp (°C)	Max NPP	extinction age (Ma)
Australopithecus anamensis	8.5	16.7	73.7	561.7	30.4	699.3	3.85
Australopithecus afarensis	13.4	22.0	48.3	465.3	29.8	431.3	3.00
Paranthropus boisei	0.6	-15.5	0.0	2000.0	31.2	909.3	1.30
Paranthropus robustus	6.0	9.4	0.2	1094.2	33.2	981.9	0.96
Homo habilis	7.7	13.9	22.6	782.6	30.8	848.8	1.39
Homo ergaster	0.0	-12.3	0.0	963.3	30.2	1113.7	0.88
Homo erectus	0.0	-28.2	0.0	586.1	29.2	1093.4	0.11
Homo heidelbergensis	0.0	-33.6	0.0	1105.5	35.6	1458.0	0.20
Homo neanderthalensis	5.7	16.6	58.9	877.6	29.6	852.4	0.04
Homo sapiens	14.2	9.8	333.9	339.9	24.0	456.6	0.04

B

Node	descendants	minPrec	minTemp (°C)	Min NPP	maxPrec (mm)	maxTemp (°C)	Max NPP	mean age (Ma)
11	hominins	12.5	20.0	52.6	513.0	29.9	490.8	4.96
12	*Homo* spp.	6.0	3.8	15.3	946.7	31.5	894.0	2.92
13	*Homo* spp. without *H. habilis*	4.8	0.0	8.8	1032.7	31.8	959.1	2.32
14	MHS	0.7	-21.1	1.7	904.8	31.7	1182.6	0.99
15	MHS without *H. heidelbergensis*	0.2	-23.7	0.5	878.8	31.5	1204.0	0.48
16	*H. ergaster* plus *H. erectus*	4.8	0.7	6.9	1080.7	31.9	960.1	1.91
17	australopiths	12.6	20.5	55.6	499.8	29.8	482.2	4.49
18	*Australopithecus* spp.	12.7	20.8	54.5	492.9	29.8	475.6	4.24
19	*Paranthropus* spp.	12.2	19.7	67.5	522.5	29.5	509.8	3.83

Table S1. A. Paleoclimatic estimates for the hominin species in the tree. B. Reconstructed climatic values at the tree nodes. Related to Figures 1 - 3.

A

Species	minPrec (mm)	minTemp (°C)	Min NPP	maxPrec (mm)	maxTemp (°C)	Max NPP	extinction age (Ma)
Australopithecus anamensis	13.5	22	48.3	465.3	29.8	431.3	3.85
Australopithecus afarensis	8.5	16.7	81.5	538.4	30.2	676.7	3
Paranthropus boisei	5.7	16.6	58.9	877.6	29.6	852.4	1.3
Paranthropus robustus	14.2	9.8	333.9	340	24	456.6	0.96
Homo habilis	7.7	13.9	22.6	782.56	30.8	848.8	1.39
Homo ergaster	6	9.4	0.2	1094.2	33.2	981.9	0.88
Homo erectus	0.6	-15.5	0	2000	31.2	909.3	0.11
Homo heidelbergensis	0	-10.6	0	878.5	29.4	1016.3	0.2
Homo neanderthalensis	0	-25.5	0	498.9	26	921.7	0.04
Homo sapiens	0	-29.6	0	952.9	32.8	922.8	0.04

B

Node	descendants	minPrec	minTemp (°C)	Min NPP	maxPrec (mm)	maxTemp (°C)	Max NPP	mean age (Ma)
11	hominins	12.4	20.3	53.4	510.4	29.8	490.9	4.96
12	*Homo* spp.	6	4.4	15.6	925.9	31	839.8	2.94
13	*Homo* spp. without *H. habilis*	4.8	0.7	9.2	1009.2	31.2	892.1	2.32
14	MHS	0.7	-18.6	1.6	809.1	29.6	945.3	0.98
15	MHS without *H. heidelbergensis*	0.2	-20.9	0.7	783.6	29.4	949.9	0.48
16	*H. ergaster* plus *H. erectus*	4.8	1.1	7.4	1060.8	31.5	904.1	1.92
17	australopiths	12.5	20.7	56.6	497.4	29.7	484.9	4.49
18	*Australopithecus* spp.	12.6	21.1	55.6	490.3	29.8	479.4	4.24
19	*Paranthropus* spp.	12.1	19.9	69.8	517.7	29.5	510.2	3.84

Table S2. A. Paleoclimatic estimates for the hominin species in the tree. B. Reconstructed climatic values at the tree nodes after subsampling the most abundant species. Related to Figures 1 - 3.

A

Species	minPrec (mm)	minTemp (°C)	Min NPP	maxPrec (mm)	maxTemp (°C)	Max NPP	extinction age (Ma)
Australopithecus anamensis	16	22.6	46.2	457.7	29.7	423.7	3.85
Australopithecus afarensis	10.5	17.1	76.7	490.6	29.8	625.7	3
Paranthropus boisei	5.1	15.7	54.4	657.8	29.4	648.7	1.3
Paranthropus robustus	13.9	8.4	330	332.5	23.6	446.9	0.96
Homo habilis	5.4	14.2	26.8	553.8	29.9	678.4	1.39
Homo ergaster	6.7	10	0.3	652.1	29.7	707.9	0.88
Homo erectus	0.6	-16.5	0	896.8	28.3	752.5	0.11
Homo heidelbergensis	5.4	14.2	26.8	553.8	29.9	678.4	0.2
Homo neanderthalensis	0	-17.3	0	380.6	24.9	706.5	0.04
Homo sapiens	0	-27.9	0	383.5	22.8	702.4	0.04

B

Node	descendants	minPrec	minTemp (°C)	Min NPP	maxPrec (mm)	maxTemp (°C)	Max NPP	mean age (Ma)
11	hominins	14.6	20.7	50.9	468.7	29.5	461	4.96
12	*Homo* spp.	5.8	3.1	15.1	579.1	28.7	658.8	2.89
13	*Homo* spp. without *H. habilis*	4.8	-0.1	10.3	594.3	28.5	679.2	2.33
14	MHS	0.9	-21.5	2.3	479.5	25.9	690.4	1.03
15	MHS without *H. heidelbergensis*	0.3	-24.9	1.1	458.6	25.5	692.5	0.48
16	*H. ergaster* plus *H. erectus*	4.9	0.6	7.8	617.5	28.7	687.2	1.89
17	australopiths	14.8	21.2	54	465.2	29.5	459.1	4.47
18	*Australopithecus* spp.	14.9	21.4	53.1	463.8	29.6	457.6	4.25
19	*Paranthropus* spp.	13.7	19.9	68.2	477.3	29.2	477.7	3.74

Table S3. A. Paleoclimatic estimates for the hominin species in the tree. B. Reconstructed climatic values at the tree nodes after removing the first decile of the climatic variable values. Nodes refer to the node number in the tree. Nodes refer to the node number in the tree. Related to Figures 1 - 3.

A

Species	minPrec (mm)	minTemp (°C)	Min NPP	maxPrec (mm)	maxTemp (°C)	Max NPP	extinction age (Ma)
Australopithecus anamensis	0.6	18.9	18.2	718.5	32.5	1010.7	3.85
Australopithecus afarensis	0	16.6	0	904.5	34.4	1310.5	3
Paranthropus boisei	0.1	15.3	93.7	809.4	29.8	968.5	1.3
Paranthropus robustus	1.7	9.2	113	370	26.2	610.6	0.96
Homo habilis	0	11.3	24.4	797.7	30.9	1001.2	1.39
Homo ergaster	0	-4.3	0	732.5	35.9	899	0.88
Homo erectus	0	-22.3	0	1290	33.6	833.4	0.11
Homo heidelbergensis	0	-23.3	0	1069	34.7	873	0.2
Homo neanderthalensis	0	-32.5	0	834.5	31.3	626.2	0.04
Homo sapiens	0	-35.2	0	1050.4	33.4	797.6	0.04

B

Node	descendants	minPrec	minTemp (°C)	Min NPP	maxPrec (mm)	maxTemp (°C)	Max NPP	mean age (Ma)
11	hominins	0.5	17	19.2	736	32.6	1016.6	4.96
12	*Homo* spp.	0.1	-3.7	9.5	854	33.3	912.4	2.87
13	*Homo* spp. without *H. habilis*	0.1	-7.5	6.8	872.6	33.6	891.5	2.34
14	MHS	0	-26.6	1.1	967.1	33.2	786.5	1.03
15	MHS without *H. heidelbergensis*	0	-29.3	0.3	988.9	33.2	778.6	0.49
16	*H. ergaster* plus *H. erectus*	0	-7.7	5.4	870.9	33.9	890.1	1.91
17	australopiths	0.5	17.7	20	733.8	32.5	1024	4.47
18	*Australopithecus* spp.	0.5	17.9	19.1	734.5	32.6	1028.1	4.25
19	*Paranthropus* spp.	0.6	17.2	31.1	722	32	999.7	3.77

Table S4. A. Paleoclimatic estimates for the hominin species in the tree. B. Reconstructed climatic values at the tree nodes after randomly shuffling the fossil occurrence data within the biogeographical domain of individual species. Nodes refer to the node number in the tree. Related to Figures 1 - 3.

A

Species	minPrec (mm)	minTemp (°C)	Min NPP	maxPrec (mm)	maxTemp (°C)	Max NPP	extinction age (Ma)
Australopithecus anamensis	13.4	22.0	48.3	465.3	29.8	431.3	3.85
Australopithecus afarensis	8.5	16.7	73.7	561.7	30.4	699.3	3.00
Paranthropus boisei	5.7	16.6	58.9	877.6	29.6	852.4	1.30
Paranthropus robustus	14.2	9.8	333.9	339.9	24.0	456.6	0.96
Homo habilis	7.7	13.9	22.6	782.6	30.8	848.8	1.39
Homo ergaster	6.0	9.4	0.2	1094.2	33.2	981.9	0.88
Homo erectus	0.6	-15.5	0.0	2000.0	31.2	909.3	0.11
Homo heidelbergensis	0.0	-12.3	0.0	963.3	30.2	1113.7	0.20
Homo neanderthalensis	0.0	-28.2	0.0	586.1	29.2	1093.4	0.04
Homo sapiens	0.0	-33.6	0.0	1105.5	35.6	1458.0	0.04

B

Node	descendants	minPrec	minTemp (°C)	Min NPP	maxPrec (mm)	maxTemp (°C)	Max NPP	mean age (Ma)
11	hominins	12.5	20.0	52.6	513.0	29.9	490.8	4.96
12	*Homo* spp.	6.0	3.8	15.3	946.7	31.5	894.0	2.92
13	*Homo* spp. without *H. habilis*	4.8	0.0	8.8	1032.7	31.8	959.1	2.32
14	MHS	0.7	-21.1	1.7	904.8	31.7	1182.6	0.99
15	MHS without *H. heidelbergensis*	0.2	-23.7	0.5	878.8	31.5	1204.0	0.48
16	*H. ergaster* plus *H. erectus*	4.8	0.7	6.9	1080.7	31.9	960.1	1.91
17	australopiths	12.6	20.5	55.6	499.8	29.8	482.2	4.49
18	*Australopithecus* spp.	12.7	20.8	54.5	492.9	29.8	475.6	4.24
19	*Paranthropus* spp.	12.2	19.7	67.5	522.5	29.5	509.8	3.83

Table S5. A. Paleoclimatic estimates for the hominin species in the tree. B. Reconstructed average climatic values at the tree nodes. Related to Figures 1 - 3.

Transparent Methods

Fossil occurrence and phylogenetic data

The human fossil record dataset we used includes 2,597 hominin occurrences associated with 727 archaeological sites. The time range of our record spans from the first occurrence of australopiths in East Africa dated to some 4.2 Ma, to the definitive advent of *H. sapiens* in Eurasia almost coincident with the demise of *H. neanderthalensis* dated some to 0.040 Ma (see Dataset S1, Raia et al., 2020). We excluded hominin with stratigraphically or geographically restricted fossil record which prevents drawing realistic inference about their climatic niche limits. The species in the database are 2 *Australopithecus* (*A. afarensis* and *A. africanus*), 2 *Paranthropus* (*P. robustus* and *P. boisei*) and 6 *Homo* species (*H. sapiens, H. neanderthalensis, H. heidelbergensis, H. erectus, H. ergaster* and *H. habilis*).

For each fossil occurrence included in the dataset, we recorded paleo-latitude and paleo-longitude, the archaeological layer yielding the remains, and the absolute age of the dated sample. Where available, we also included information about which sample was used for dating the relative lab code. Radiocarbon dates were calibrated using Intcal13 calibration curve for the Northern hemisphere, shcal13 curve for the Southern hemisphere, and marine13 curve for marine samples. Age estimates come with uncertainty. Time averaging of the archaeological layers adds to this uncertainty. To account for this, for each archaeological site (or layer) age estimate we retrieved from the collected estimates the minimum age and the maximum age (calculated according to individual estimates and their respective confidence intervals).

Environmental predictors

Environmental predictors were generated using a paleoclimate emulator (Holden et al., 2019). The method applies Gaussian process emulation of the singular value decomposition of ensembles of runs from the intermediate complexity atmosphere-ocean GCM PLASIM-GENIE with varied boundary-condition forcing (CO_2, orbit and ice-volume). Spatial fields of i) minimum

temperature of the coldest quarter of the year (hereafter, “MinTemp”) , ii) maximum temperature of the warmest quarter (hereafter, “MaxTemp”), iii) minimum precipitation of the driest quarter (hereafter, “MinPrec”), iv) maximum precipitation of the wettest quarter (hereafter, “MaxPrec”), and v) yearly net primary productivity (hereafter, “NPP”) are then emulated at 1,000 year intervals, driven by time-series of scalar boundary-condition forcing, and assuming the climate is in quasi-equilibrium. The emulator uses CO_2 from Antarctic ice cores for the last 800,000 years (Lüthi et al., 2008). Prior to 800 ka, and for the entire sea-level record, it uses the CO_2 and sea-level reconstructions in Stap et al. (2017). Contemporary values of the four bioclimatic variables were derived from WorldClim (Hijmans et al., 2005), while NPP observations were derived from MOD17A3H (MODIS; https://lpdaac.usgs.gov/products/mod17a3hv006/). Current bioclimatic variables and the NPP were interpolated onto the same 0.5° grid and combined with emulated anomalies. Temperature anomalies were additively combined with current temperatures, while precipitation and NPP anomalies were combined with current precipitations using a hybrid additive/multiplicative approach (Holden et al., 2019).

The native-resolution (5°) emulations have been extensively validated (Holden et al., 2019) against model inter-comparisons of the mid-Holocene, the Last Glacial Maximum, the Last Interglacial and the mid-Pliocene warm period. Glacial-interglacial variability was validated (Holden et al., 2019) against observationally based global temperature reconstructions (Köhler et al., 2010). These analyses demonstrated that PALEO-PGEM lies within the uncertainty envelope of high resolution IPCC models, which have themselves been validated against proxy data in the Mid-Holocene and Last Glacial Maximum (Braconnot et al., 2007) and the Pliocene (Haywood et al., 2013). Paleoclimate anomalies at climate model resolution (5°) were downscaled onto the observed modern climatology at 0.5° spatial resolution using bilinear interpolation. We used the entire bioclimatic predictors in order to consider the last 5 million years of human evolution.

Definition of the Climatic Niche limits for *Homo* species

For each hominin species, we built its climatic envelope (the hypervolume defined by the climatic variables), by pooling together all bioclimatic values associated to their fossil occurrences. Then, we selected the recorded minimum values for MinTemp, MinPrec, and NPP, and the maximum values for MaxTemp, MaxPrec, and NPP. We repeated this procedure over 100 replicates. At each replication, the age of each individual archaeological locality was sampled at random from the uniform distribution spanning from the estimated minimum to the estimated maximum locality age. Thus, replication accounts for both ageing uncertainty of individual archaeological layers and, correspondingly, for climatic uncertainty around the paleoclimatic estimates concerning the fossil localities. Finally, for each bioclimatic variable, we took the mean value from each resulting distribution of temperature, precipitation and NPP minima and maxima. Taken together, these mean values of bioclimatic extremes represent a conservative estimate of the climatic range realized for each hominin species during its history, avoiding putting too much faith on extreme values attached to individual replicates and locality.

Definition of the Climatic Niche limits for common ancestors in the hominin tree

The 10 species phylogenetic tree was obtained by combining the Primate (and human) phylogenetic information published in recent papers (Diniz-Filho et al., 2019; Melchionna et al., 2020; Parins-Fukuchi et al., 2019). We started by using the six climatic variables, representing the limits (minima and maxima) in temperature, precipitation and NPP. Since these variables are highly correlated to each other, we reduced covariation among variables by performing a Principal Component Analysis (PCA) on climatic variables associated with each hominin species occurrence in the fossil record. Then, we extracted the PC scores and used them as a multivariate dataset for the phylogenetic ridge regression. To estimate the rates of climatic niche limits evolution we applied the function *RRphylo* (Castiglione et al., 2018) in the R package RRphylo. The function estimates

rates and ancestral states estimates by means of phylogenetic ridge regression. PC scores were used as the response variable in *RRphylo*.

We used the PC scores estimated by *RRphylo* at each node (ancestral states) and back transformed the scores in climatic variables (MinTemp, MinPrec, min NPP, MaxTemp, MaxPrec, max NPP) to map geographically the areas associated with the corresponding climatic estimates (i.e. the area within the limits of the climatic envelope for each ancestor in the tree). The resulting map thus represents the geographic areas estimated to be climatically suitable for occupation by the hominin ancestors. To account for uncertainty around the ages of individual nodes in the hominin phylogeny, we repeated the entire procedure at each node over 100 replicates by using the 100 alternative phylogenies generated from *swapONE* function embedded in the RRphylo package. This function randomly changes the tree topology and branch lengths although it is possible to keep specific clades monophyletic. However, we accounted for a few, well-supported, monophyletic clades which are present in the hominin tree. In particular, in swapping the tree tips and moving (in time) the nodes in the tree, we kept *H. ergaster* and *H. erectus* as sister species. We similarly kept monophyletic the clade subtending to the four australopithecines in the tree, the clade representing the genus *Homo*, and the clade including *H. heidelbergensis*, *H. neanderthalensis* and *H. sapiens*. Since the inclusion of particular taxa in the data may alter significantly the result of PCA ordination (Adams et al., 2011) we repeated the swap procedure leaving one species at random out of the tree for each replicate.

Eventually, for each given species and ancestor in the tree we recorded the number of times a given geographical cell counts as climatically suitable out of the 100 replicates, thus defining an overall 'habitat quality' metric, representing the number of iterations (out of 100) a geographic cell was found habitable (i.e. fell within climatic tolerance limits) for any given species or ancestor in the tree. For each cell, habitat quality thus ranges between 0 (never suitable) to 1 (always suitable).

Measuring the association between the archaeological record and habitat quality

Climatic variables limit at the tree node represent the estimated tolerance limits for hominin ancestors. Since these values are estimated, rather than observed, to assess the association between the position of fossil localities and habitat quality for each ancestral species estimates we selected the fossil occurrences of its descendants, provided they are not included in a descending node which was itself tested. For instance, the EHS ancestor was tested by selecting the fossil occurrence of *H. habilis*, *H. erectus* and *H. ergaster*, but not *H. sapiens*, *H. neanderthalensis* and *H. heidelbergensis* which were considered only descendant to the MHS ancestor. To measure the association between climatic suitability and the presence of human species, we calculated the Area Under receiver-operator Curve (AUC) averaging over the 100 replicates. AUC theoretically ranges from 0 to 1. However, since random sampling points, (pseudoabsences) are not real absences, AUC cannot reach 1 (Jimenez-Valverde, 2012), as the maximum AUC value depends on the actual (unknown) area of distribution of the species. To obtain a null distribution of AUC values and assess significance for the real AUC, for each node in the tree we sampled 100 times as many point occurrences as with the real data (i.e. the fossil occurrences of the species descending from that node) within the biogeographic domain of the species groups (i.e. the descendants to a given node in the tree), and calculated the random AUC. To account for sampling differences between the hominin species, we further repeated the AUC computation after sampling randomly no more than 100 occurrences per species at each replicate.

Measuring rates of climatic niche limits evolution

We used the evolutionary rates provided by *RRphylo* to apply the function *search.shift* (Castiglione et al., 2018) which tests whether individual clades evolved at significantly different rates as compared to the rest of the tree. The function compares the rates attached to each branch descending from a particular node to the rates for the branches of the rest of the tree. The significance for the rate difference is assessed by means of randomization. In the case of

multivariate data, as with this particular study, the multivariate rate is computed as the 2-Norm (Euclidean) vector of the rates of individual variables.

To look for possible evolutionary trends in climatic tolerances over time we used the function *search.trend* (Castiglione et al., 2019) in the *RRphylo* R package. In *search.trend*, evolutionary rates and phenotypes (including the phenotypic estimates at the nodes) are regressed against their age and the resulting slopes compared to slopes randomly generated under the Brownian motion model of evolution, which is a model assuming no temporal trend is present in the data.

Estimating habitat quality under the Brownian motion model of evolution

To estimate and map habitat quality under the assumption that climatic niche limits evolved under a random walk model with constant variance (namely the Brownian motion model of evolution, BM) we estimated climatic niche limits for human ancestors by using the Rphylopars package in R. In Rphylopars, trait values for tree tips with missing data are assessed according to a single rate of evolution calculated for the rest of the tree and data (Bruggeman et al., 2009). Since we found a significant rate shift in niche width referring to the MHS ancestor (node 14) we derived the estimates for both this ancestor (node 14), and the ancestor of *Homo sapiens* and *Homo neanderthalensis* (node 15), pruning the tree of its descendants, and then treating the node as a species with missing data.

Supplemental references

Adams, D.C., Cardini, A., Monteiro, L.R., O'Higgins, P., and Rohlf, F.J. (2011). Morphometrics and phylogenetics: Principal components of shape from cranial modules are neither appropriate nor effective cladistic characters. J. Hum. Evol. *60*, 240–243.

Braconnot, P., Otto-Bliesner, B., Harrison, S., Joussaume, S., Peterchmitt, J-Y., Abe-Ouchi, A., Crucifix, M., Driesschaert, E., Fichefet, Th., Hewitt, C.D., et al. (2007). Results of PMIP2 coupled simulations of the Mid-Holocene and Last Glacial Maximum – Part 1: experiments and large-scale features, Clim. Past *3*, 261– 277.

Bruggeman, J., Heringa, J. and Brandt, B.W. (2009). PhyloPars: estimation of missing parameter values using phylogeny. Nucl. Acid. Res. *37*, W179-W184.

Castiglione, S., Serio, C., Mondanaro, A., Di Febbraro, M., Profico, A., Girardi, G., and Raia, P. (2019). Simultaneous detection of macroevolutionary patterns in phenotypic means and rate of change with and within phylogenetic trees including extinct species. PLoS ONE *14*, e0210101–13.

Castiglione, S., Tesone, G., Piccolo, M., Melchionna, M., Mondanaro, A., Serio, C., Di Febbraro, M., and Raia, P. (2018). A new method for testing evolutionary rate variation and shifts in phenotypic evolution. Meth. Ecol. Evol. *9*, 974–983.

Diniz-Filho, J.A.F., Jardim, L., Mondanaro, A., and Raia, P. (2019). Multiple Components of Phylogenetic Non-stationarity in the Evolution of Brain Size in Fossil Hominins. Evol. Biol. *46*, 47-59.

Haywood, A.M., Hill, D.J., Dolan, A.M., Otto-Bliesner, B.L., Bragg, F., Chan, W.-L., Chandler, M.A., Contoux, C., Dowsett, H.J., Jost, A., et al. (2013). Large-scale features of Pliocene climate: results from the Pliocene Model Intercomparison Project, Clim. Past *9*, 191–209.

Holden, P.B., Edwards, N.R., Rangel, T.F., Pereira, E.B., Tran, G.T., and Wilkinson, R.D. (2019). PALEO-PGEM v1. 0: a statistical emulator of Pliocene–Pleistocene climate. Geoscientific Model Development *12*, 5137-5155.

Jimenez-Valverde, A. (2012). Insights into the area under the receiver operating characteristic curve (AUC) as a discrimination measure in species distribution modelling. Glob. Ecol. Biogeogr. *21*, 498–507.

Köhler, P., Bintanja, R., Fischer, H., Joos, F., Lohmann, G., and Masson-Delmotte, V. (2010). What caused Earth's temperature variations during the last 800,000 years?. Quat. Sci. Rev. *21*, 129-145.

Lüthi, D., Le Floch, M., Bereiter, B., Blunier, T., Barnola, J.-M., Siegenthaler, U., Raynaud, D., Jouzel, J., Fischer, H., Kawamura, K., and Stocker, T.F. (2008). High-resolution carbon dioxide concentration record 650,000–800,000 years before present. Nature *453*, 379–382.

Melchionna, M., Mondanaro, A., Serio, C., Castiglione, S., Di Febbraro, M., Rook, L., Diniz-Filho, J.A.F., Manzi, G., Profico, A., Sansalone, G., and Raia, P. (2020). Macroevolutionary trends of brain mass in Primates. Biol. J. Linn. Soc.*129*, 14–25.

Parins-Fukuchi, C., Greiner, E., MacLatchy, L.M., and Fisher, D.C. (2019). Phylogeny, ancestors, and anagenesis in the hominin fossil record. Paleobiology *45*, 378–393.

Raia, P., Mondanaro, A., Melchionna M., Di Febbraro, M., Diniz-Filho, J.A.F., Rangel, T.F., Holden, P.B., Carotenuto, F., Edwards, N.R., Lima-Ribeiro, M.S., et al. (2020). Past extinctions of *Homo* species coincided with increased vulnerability to climatic change. One Earth in press.

Stap, L.B., Van De Wal, R.S.W., De Boer, B., Bintanja, R., and Lourens, L.J. (2017). The influence of ice sheets on temperature during the past 38 million years inferred from a one-dimensional ice sheet-climate model. Clim. Past *13*, 1243-1257.